LA-UR- 08-5052

Approved for public release;
distribution is unlimited.

Title: Performance and Durability of PEM Fuel Cells Operated at Sub-Freezing Temperatures

Author(s):
Rangachary Mukundan
John R. Davey
Roger W. Lujan
Jacob Spendelow
Yu Seung Kim
Daniel Hussey
David Jacobson

Intended for:
ECS Transactions
Proton Exchange Membrane Fuel Cells 8

Los Alamos
NATIONAL LABORATORY
EST. 1943

Form 836 (7/06)

Performance and Durability of PEM Fuel Cells Operated at Sub-Freezing Temperatures

Rangachary Mukundan[a], John R. Davey[a], Roger W. Lujan[a], Jacob S. Spendelow[a], Yu Seung Kim[a], Daniel S. Hussey[b], David L. Jacobson[b], Muhammad Arif[b], and Rodney L. Borup[a]

[a]Los Alamos National Laboratory, MS D429, MPA-11, Los Alamos, NM 87545
[b]National Institute of Standards and Technology (NIST), Center for Neutron Research, 100 Bureau Drive, MS 8461, Gaithersburg, MD 20899

The effect of MEA preparation on the performance of single-PEM fuel cells operated at sub-freezing temperatures is presented. The cell performance and durability are dependent on the MEA and are probably influenced by the porosity of the catalyst layers. When a cell is operated isothermally at -10 °C in constant current mode, the voltage gradually decreases over time and eventually drops to zero. AC impedance analysis indicated that the rate of voltage loss is initially due to an increase in the charge transfer resistance and is gradual. After a period, the rate of decay accelerates rapidly due to mass transport limitations at the catalyst and/or gas diffusion layers. The high frequency resistance also increases over time during the isothermal operation at sub-freezing temperatures and was a function of the initial membrane water content. LANL prepared MEAs showed very little loss in the catalyst surface area with multiple sub-freezing operations, whereas the commercial MEAs exhibited significant loss in cathode surface area with the anode being unaffected. These results indicate that catalyst layer ice formation is influenced strongly by the MEA and is responsible for the long-term degradation of fuel cells operated at sub-freezing temperatures. This ice formation was monitored using neutron radiography and was found to be concentrated near cell edges at the flow field turns. The water distribution also indicated that ice may be forming mainly in the GDLs at -10 °C and could be concentrated in the catalyst layer at -20 °C.

Introduction

The durability of polymer electrolyte membrane (PEM) fuel cells operated at sub-freezing temperatures has received increasing attention in recent years.[1] The Department of Energy's PEM fuel cell stack technical targets for the year 2010 include un-assisted startup from –40°C and startup from -20 °C ambient in as low as 30 seconds with < 5MJ energy consumption. Moreover, the sub-freezing operations should not have any impact on achieving other technical targets including 5000 hours durability. We have previously characterized the performance of both cloth (E-tek) and paper (SGL) GDLs and reported that the paper GDLs show lower tolerance to sub-freezing temperatures.[2] We have also reported the performance of LANL (Los Alamos National Laboratory) prepared MEAs at -10 °C where ice formation results in mass transport limitations[3]. Our results also

revealed that this ice formation did not result in significant irrecoverable losses once the cell was thawed and operated at elevated temperatures (80 °C)[3].

Literature studies have shown that PEM fuel cells are capable of self-starting from sub-ambient temperatures as low as -20 °C without any external heating[4]. This is primarily achieved by drying out the water in the cell hardware during shutdown, which prevents ice formation from blocking the flow fields during startup[4,5]. While the fuel cell is operated at sub-freezing temperatures, the water generated at the cathode will tend to form ice that results in a loss in performance of the fuel cell. The measured (AC impedance) charge transfer resistance during a cold start from -10 °C has been shown to increase with time providing evidence for ice build up in the catalyst layer[3,6]. This catalyst layer ice formation at an operating temperature of -20 °C has been quantified as a function of the initial membrane water content (λ), and current density with longer operating times (more capacity for water/ice formation) being demonstrated at lower initial λs, and lower operating currents[7]. Cyclic voltammograms have shown that there is significant loss in surface area of the catalyst layer due to this ice formation that also results in irrecoverable losses once the fuel cell is heated up to the operating temperature[8]. Therefore a successful startup of the cell requires that temperatures above freezing be achieved before the ice formation inhibits cell performance to a point where the cell cannot generate sufficient heat. While this has been successfully demonstrated in stacks, it is difficult to achieve in single cells that have a relatively large thermal mass compared to the heat they generate. In this study we explore the characteristics of single cells operated at -10 °C and -20 °C using AC impedance spectroscopy, cyclic voltammograms (CVs), polarization curves (VIRs) and neutron radiography to elucidate ice formation and its effect on fuel cell performance at sub freezing temperatures. We also report the effect of MEA structure on sub-freezing performance and durability issues arising from repeated isothermal starts at sub-freezing temperatures.

Experimental

Fuel Cell Testing

Two different fuel cell configurations were studied to illustrate the effect of MEA preparation on sub-freezing performance and durability. The first set of cells were assembled with Nafion® 1135 membranes having 0.2 mg cm^{-2} Pt (E-Tek 20% Pt/C) areal density at the cathode and anode and E-tek cloth GDLs. The second set of cells were assembled with a GORE™ PRIMEA® 57 series MEA with 0.2 mg cm^{-2} Pt areal density at the cathode and 0.1 mg cm^{-2} Pt areal density at the anode and SGL carbon paper (Sigracet® GDL 24 series) GDLs[9,10]. Special single cells with serpentine graphite flow fields and cooling loops machined into the metal end plates were used in order to cool the 50 cm^2 MEAs to -10 °C and -20 °C. Polarization curves with high frequency resistance measurements (VIRs) and AC impedance spectra were obtained using a fuel cell test station from Fuel Cell Technologies Inc. Cathode CVs (from 0.1 to 1.0 V @ 20 – 60 mV sec^{-1}) were performed using either Pine or PAR potentiostats at 500 cm^3 min^{-1} of N_2 and H_2 at the cathode and anode respectively. The cells were first operated at 0.6 V at 80 °C with air (2.0 stoich) and H_2 (1.2 stoich) at 100% inlet RHs and 30 psi back pressure. The cells were then purged using N_2 gas (< 5000cc/min for < 3 minutes) at atmospheric pressure and cooled down to sub freezing temperatures. Dry H_2 and dry air (at 500 cc min^{-1}) were then introduced into the anode and cathode of the cells and their

performance was monitored isothermally at sub freezing temperatures at various constant current densities. Cyclic voltammograms were obtained before and after the application of current and were used to determine the electrochemical catalyst surface area (H2 desorption peak)[3,8]. AC impedance spectra or HFR measurements were performed during the sub-freezing operation to illustrate the origin of the voltage loss.

Neutron Imaging

The neutron imaging was performed at the NIST Center for Neutron Research (NCNR) on thermal beam tube 2. The measurements were conducted using beam #1 and aperture #4 with a fluence rate of 2×10^7 neutrons cm^{-2} sec^{-1}. The details of the imaging and the cooling chamber have been described previously[3]. These experiments were performed on a 50 cm^2 active area cell with single serpentine channels machined in an aluminum (coated with nickel and gold) flow field/current collector plates. The cells were cooled in an environmental chamber to -10 °C and -20 °C where the imaging was performed.

The neutron image analysis was performed using the IDL programming language and a dry reference image as described by Hickner et al.[11]. The dry image was the average of 1800 images that were obtained for ½ hour after drying the cell at 80 °C in flowing dry N_2 gas for 2 hours. Masks (to scale) were made to represent the lands, channels and active area of the cells. The land masks and channel masks were superimposed on the dry image to ensure that the correct area of the image was being analyzed. The positioning of these masks were such that the land/channel edges were accounted for only in the active area mask, which included the entire active area excluding the inlet and outlets. Therefore the land water content represents the water from the MEA components in the middle (≈ 80%) of the land area and the channel water content represents the water from the middle (≈ 80%) of the anode and cathode flow channels and the MEA components in-between. The images collected at sub-freezing temperatures were averaged over 5 seconds (to reduce noise) and their water/ice content determined with respect to the dry image (at the same temperature) using Beer-Lambert's law[3,10].

Results and Discussion

Operation at sub-freezing temperatures:

The performance of 2 different single cells operated at -10 °C, with a Gore™ and a LANL MEA are illustrated in Figures 1a and 1b respectively. It is seen that the cell voltage drops as expected, due to ice formation at the cathode inhibiting further electrochemical reaction. The constant current operations (Fig 1a.) illustrate the wide variability in the amount of charge (871 to 1270 Coulombs) that can be passed before the voltage decays to zero. This charge represents the water/ice carrying capacity of the cell at sub-freezing temperatures and as previously illustrated is a function of initial membrane water content (λ) and current density[7]. However, unlike the measurements at -20 °C[7], these results actually indicate a decrease in the amount of charge that can be passed as the cell water content is decreased. For example, in start #1 the initial voltage at a current density of 0.02 A cm^{-2} is 0.81 V and the charge capacity is 1270 Coulombs whereas in start #5, the initial voltage was 0.764 V and the charge capacity is only 958 Coulombs. These results indicate that the nature of ice formation at -10 °C and – 20°C

a)

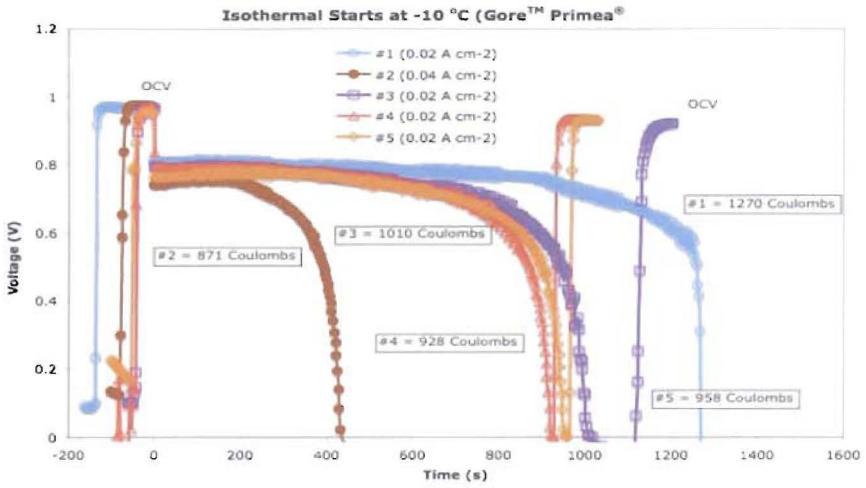

b)

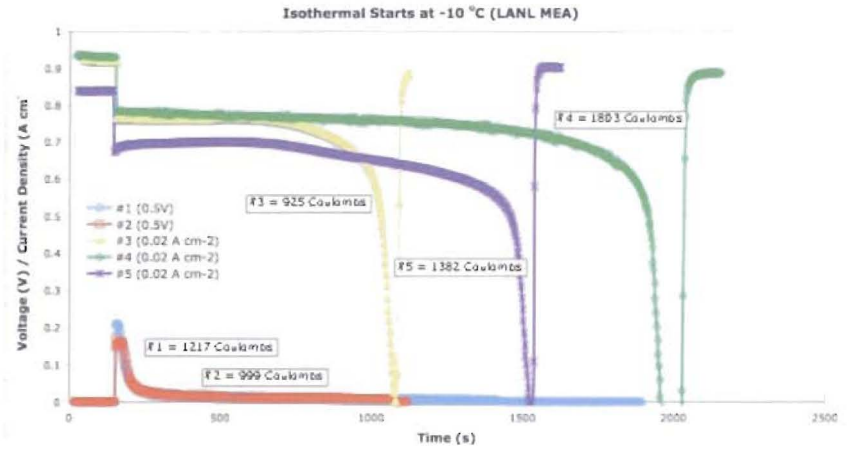

Figure 1. The performance of 2 cells operated in 500 cc min^{-1} of dry H_2 and air at constant temperature of -10 °C using a) Gore™ Primea® MEA and b) LANL MEA

may be different. However, the variability in the experiments is too large to make any conclusions. The influence of current density is illustrated in Fig 1 b., where the charge capacity varies from 925 to 1803 Coulombs and is not affected significantly by the mode of operation. For example, in the constant voltage (0.5 V) starts (#1 and #2) where the current density reaches 0.2 A cm^{-2}, a ten fold increase over the constant current starts (0.02 A cm^{-2}), the charge capacity is not significantly decreased. These results tend to indicate that the total ice/water capacity of the cell at -10 °C is not significantly influenced by either the current density or initial cell water content within the uncertainty of the experiments.

The AC impedance spectra obtained during the constant current starts is illustrated in Fig. 2 for three different starts. Figs. 2 a) and b) are data from a Gore™ MEA that was initially dried at 80 °C for 2 minutes (a) and 20 minutes (b). The MEA dried for 2 minutes showed a lower initial HFR of 0.26 Ω cm^2 when compared to the cell that was

a)

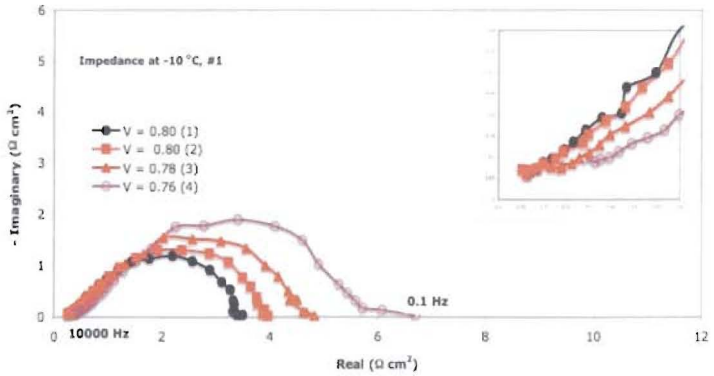

b)

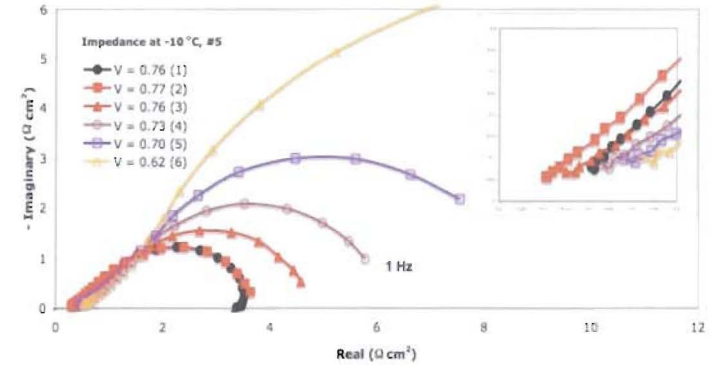

c)

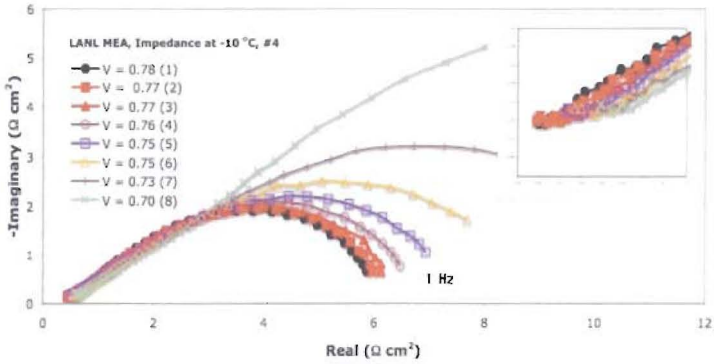

Figure 2. The AC impedance spectra obtained from 3 different starts of a) Gore^{TM} MEA dried for 2 min. at 80 °C, Gore^{TM} MEA dried for 20 min. at 80 °C, LANL MEA dried for 2 min. at 80 °C.

dried for 20 minutes (HFR = 0.42 Ω cm^2). The wetter MEA showed a steady increase in HFR to 0.53 Ω cm^2 before voltage failure while the drier MEA showed an initial drop in HFR to 0.31 Ω cm^2 followed by an increase to 0.48 Ω cm^2 before voltage failure. These results indicate that at least part of the generated water is used to hydrate the membrane, while the rest forms ice resulting in an increase in the low frequency component of the impedance spectra. The increase in HFR can be attributed to either a loss in electronic conductivity of the catalyst layer (due to ice formation moving the carbon particles

further apart) or an increase in the interface (catalyst/MEA or MPL/Catalyst) resistances. The results from a LANL MEA are shown in Fig. 2c and exhibit a similar behavior to the Gore^{TM} MEAs. The initial HFR is slightly higher (0.45 Ω cm^2), consistent with the use of a thicker membrane. Moreover, the catalyst layer resistance including the sheet resistance (proton conductivity in the catalyst layer) is higher, indicative of a thicker less optimized catalyst layer. Equivalent circuit analysis using two parallel RC circuits connected in series, one representative of charge transfer resistances and another of mass transfer resistances, indicated a steady increase in the charge transfer resistance followed by a rapid increase in the mass transfer resistance. The increase in charge transfer resistance could be due to the coupling of the proton and electron transport resistances to the charge transfer process. The increase in mass transport resistance is simply due to the fact that ice formation in the pores of the catalyst layer/GDL increases the tortuocity for gas diffusion to the 3-phase interface. This is consistent with the voltage decay curves in Fig. 1 that exhibit a steady decline followed by a rapid fall to voltage failure.

The cyclic voltammograms obtained before and after the sub-freezing starts indicated that there was no loss in catalyst surface area even when the cell was completely clogged with ice and no more current could be obtained from the cell. This is illustrated for a cold start operation on the Gore^{TM} MEA at -20 °C (Figure 3).

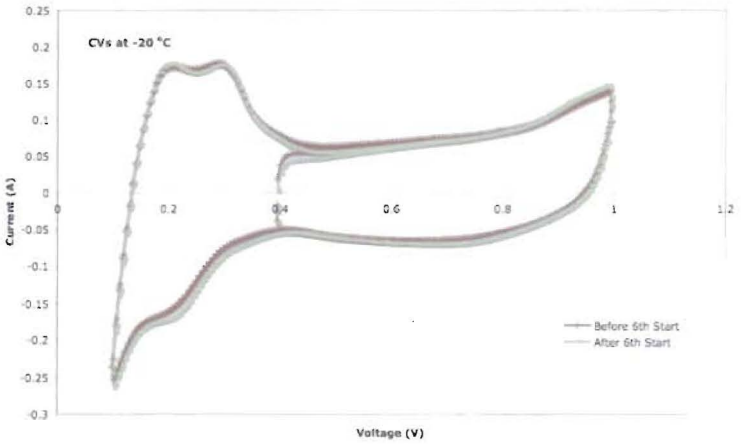

Figure 3. Cyclic voltammograms (at -20 °C) before and after a constant current operation to voltage failure.

Durability: operation at sub-freezing temperatures:

The durability of the LANL and Gore^{TM} MEAs to sub-freezing operations is compared in Fig. 4, where the initial polarization curves of the two cells are compared to those taken under identical conditions after 5 starts at -10 °C. The LANL MEA showed very little change in performance while the Gore^{TM} MEA exhibiting a slight decay in performance especially at the high current densities. These results indicate that the mass transport resistance in the cell using the Gore^{TM} MEA is increased due to ice formation during the sub-freezing operations. This is consistent with impedance curves (not shown) at the high current densities that show an increase in the low frequency resistance of the cell using the Gore^{TM} MEA with successive operations at -10 °C. On the other hand the impedance curves taken under similar conditions for the LANL MEA show very little change in the low frequency resistance. It should be noted that the cell using the Gore^{TM} MEA used paper GDLs, whereas the cell with the LANL MEA used cloth GDLs.

Moreover, our previous results had also indicated that the paper GDLs may undergo faster degradation when subjected to ice formation.

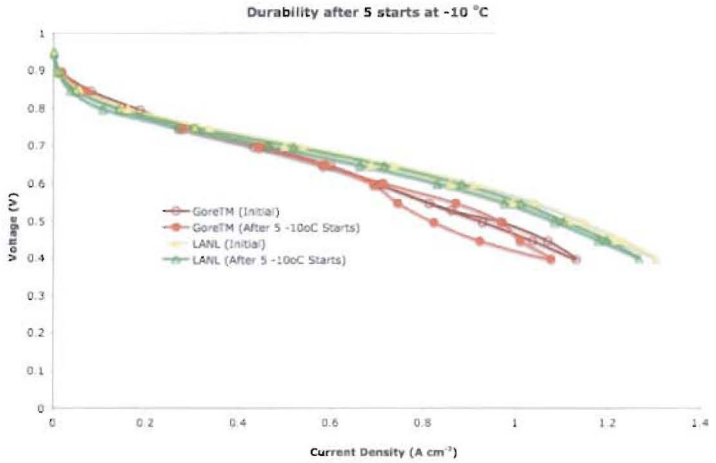

Figure 4. Polarization curves of Gore^{TM} and LANL MEAs subjected to 5 isothermal operations at -10 °C.

To distinguish between changes in the MEA versus changes in the GDL, cyclic voltammograms obtained after each successive operation at -10 °C were analyzed. This is illustrated in Fig. 5 where the cathode CVs for the LANL MEA before the first cold start

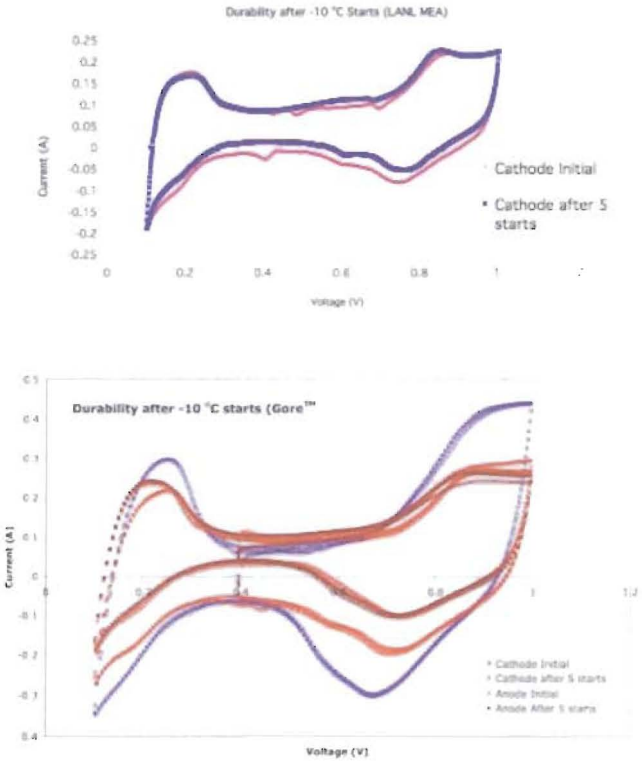

Figure 5. CVs before and after 5 operations at -10 °C for the LANL and Gore^{TM} MEAs

operation and after the 5th cold start operation are compared. There is very little change in the electrochemical catalyst surface area (ECSA) after 5 cold start operations at -10 °C.

However, the CVs performed on the Gore^{TM} MEA exhibit a significant loss (> 50% loss) in the ECSA at the cathode. On the other hand there is no loss in the ECSA at the anode of that same cell. These results indicate that the cathode catalyst layer on the Gore^{TM} MEAs is affected significantly more than the catalyst layer on the LANL MEA. This helps reconcile some of the differences observed in the literature where Ge et al.[8] reported a loss in ECSA whereas Mukundan et al.[3] reported no loss in ECSA after cold start operations at -10 °C and -20 °C. This illustrates the importance of the catalyst layer morphology to the durability of PEM fuel cells operated at sub-freezing temperatures. One possible explanation could be the fact that the water may not freeze in a catalyst layer with very small pore sizes, while it will freeze in a catalyst layer with larger pores (not enough depression in the freezing point). Ishikawa et al. have reported that the water in the catalyst layer of their MEA did not freeze at -10 °C and was present as a super-cooled liquid state that only froze on the surface after warming to 0 °C[12]. Neutron imaging of this water/ice was performed to confirm this hypothesis.

Neutron imaging of ice formation:

The water/ice content at sub-freezing temperatures was quantitatively determined using neutron radiography. These results are similar to our previously published preliminary results[3] where quantitative agreement was obtained between the observed and calculated (from the current) water contents. The experiments were further extended to include different starting membrane water contents, current densities and temperatures. These results (Fig. 6) indicated that the high frequency resistance initially drops due to membrane hydration and then steadily increases with time due to ice formation in the

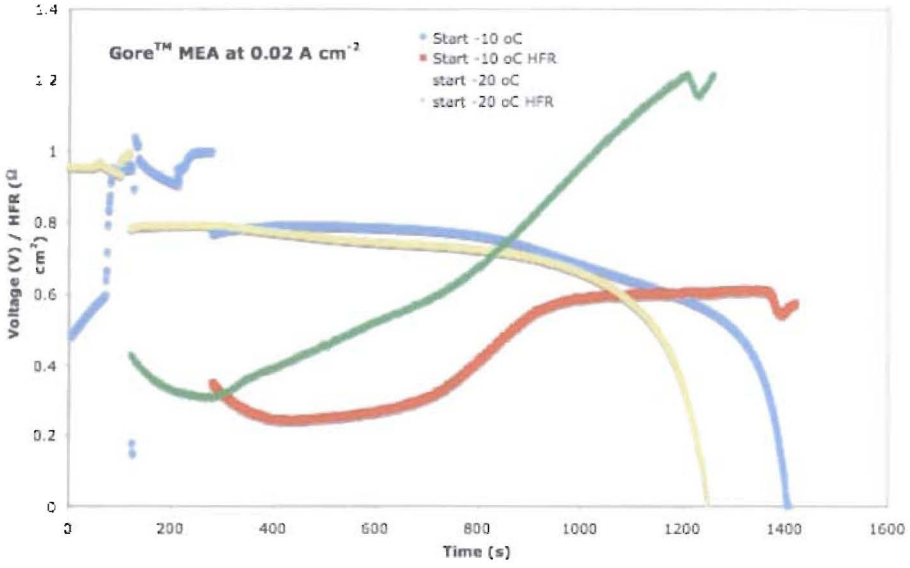

Figure 6. Performance of 2 cells (Gore^{TM} MEA) at -10 °C and -20 °C during constant current operations (I = 0.02 A cm^{-2})

catalyst/GDL layers. However, during the -10 °C start, the increase in HFR stopped and showed a plateau after a certain amount of ice formation. This plateau also corresponded to the point at which the voltage decay started to accelerate. Neutron images obtained during these starts were analyzed in order understand this phenomenon.

The water content over the lands and channels of the cell during these two operations is plotted in Figure 7, where there is slightly more initial water in the cell operated at -20 °C than the cell operated at -10 °C. When operated at -20 °C, the water content increases at almost the same rate over the lands and the channels. The land has slightly more water initially (the drying is more effective over the channels in removing water) and after

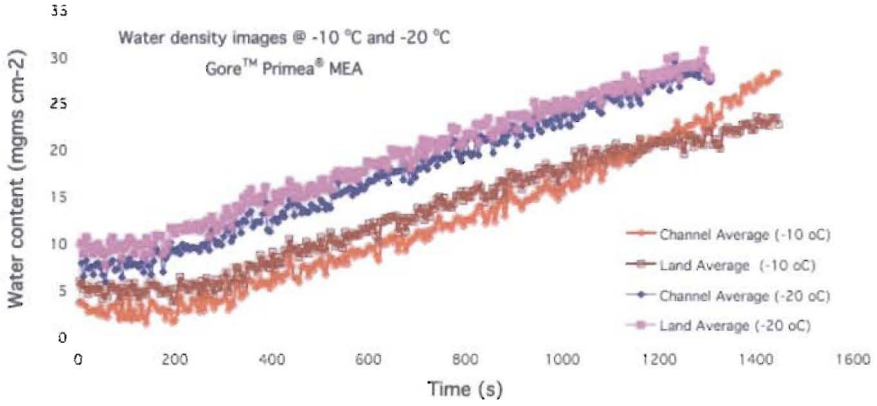

Figure 7. Calculated water contents during the operations shown in Fig. 6.

operating at 0.02 A cm^{-2} for ≈ 1100 seconds the lands and channels have approximately the same water content. This indicates that the current distribution over the channels may be slightly greater than the current distribution over the lands, consistent with easier gas transport. The more dramatic change is seen during the operation at -10 °C, where the water over the lands does not increase at the same rate throughout the experiment. For example, the open squares indicate a sharp decrease in the rate of water/ice accumulation over the lands at approximately 900 seconds. This time corresponds to the start of the plateau region in the HFR in Fig. 6. This correlation between the water accumulation in the neutron imaging and the HFR measurements confirms our hypothesis that at -10 °C liquid water is present in the catalyst layer and freezes only in the GDLs or flow channels. Initially this water freezes in the pores of the GDL evenly above the lands and channels. However, as the tortousity increases the gas access to the regions above the land decreases and the current and therefore ice formation is limited to the regions above the channels until this ice completely blocks reactant access resulting in voltage failure. This also indicates that the reason for the increasing HFR is ice formation over the lands resulting in increased contact resistances probably at the GDL/catalyst or GDL/flowfield interfaces. The absence of this HFR plateau in the -20 °C start in Fig. 6 could indicate that at such low temperatures, the ice formation is different from that at -10 °C, with ice possibly freezing more in the catalyst layers. Further experiments using the high-resolution detector at NIST and a cross-section cell are planned to confirm these observations.

The colorized images of the water contents during the -20 °C start is shown in Fig. 8, where the water density from the first 260 seconds and the last 260 seconds of operation have been averaged. This shows that the initial water content distribution is very non

uniform and may help explain some of the variability observed in our sub-freezing experiments. Here the drying was performed for 2 minutes using high (1000 sccm) flows

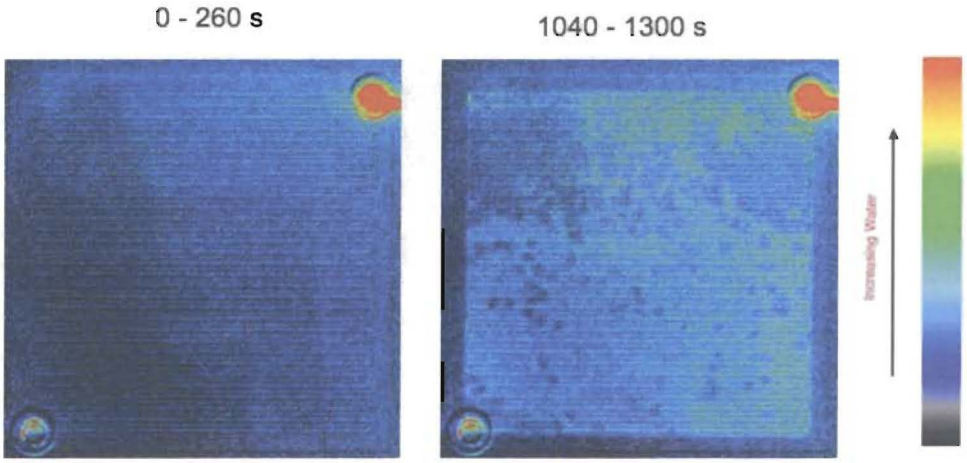

Figure 8. Water density images before and after a constant current (0.02 A cm^{-2}) operation at -20 °C.

of dry N_2 on the cathode and anode side and cell was cooled with cold air blowing from one side of the cell to another. The water is concentrated at the right side of the cell, indicating that temperature gradient driven water redistributions may have a role to play in determining the initial state of the cell. More experiments with thermocouples at various portions in the cell need to be performed to understand this phenomenon.

Conclusions

When single PEM fuel cells are subjected to iso-thermal operation at -10 °C and – 20 °C ice formation results in a loss in voltage at constant current density. Neutron imaging revealed that the ice distribution is very uneven and is concentrated near the turns in the serpentine pattern of the flow field. The distribution of the ice with respect to the lands and channels of the flow field at -10 °C and -20 °C indicates that the water may not be freezing in the catalyst layer at – 10 °C due to the freezing point depression in nanometer size pores of the catalyst layer. Performance loss during sub-freezing operations is associated with a slow increase in the kinetic resistance followed by a steep increase in the mass transport limitation. The high frequency resistance was also found to increase and this increase was closely coupled to ice formation over the land and associated increases in contact resistance. The durability of single-cells that were subjected to multiple (up to 5) isothermal operations at sub-freezing temperatures is dependant on the type of MEA. The LANL prepared MEAs showed negligible loss in catalyst surface area and minimal degradation in their performance at 80 °C. However the Gore™ MEAs showed a significant loss (> 50%) in the cathode catalyst surface area over 5 starts at -10 °C. This loss was associated with increasing mass transport resistance and decreasing performance especially at high current densities.

Acknowledgments

This work was supported by the Office of Hydrogen Fuel Cells and Infrastructure Technologies at the U.S. Department of Energy-Energy Efficiency and Renewable

Energy. This work was also supported by the U.S. Department of Commerce, the NIST Ionizing Radiation Division, the Director's Office of NIST, the NIST Center for Neutron Research, and the Department of Energy through interagency agreement no. DE-AI01-01EE50660.

References

1. R. Borup, J. Meyers, B. Pivovar, et al., *Chemical Reviews*; **107(10)**, 3904 (2007).
2. R. Mukundan, Y. S. Kim, F. Garzon, B. Pivovar, *ECS Transactions*, ***1(E)***, 403 (2005).
3. R. Mukundan, Y. S. Kim, T. Rockward, J. R. Davey, B. Pivovar, D. Hussey, D. Jacobson, M. Arif, R. Borup, *ECS Transaction*, **11(1)**, 411 (2007).
4. *Fuel Cell Operations at Sub-Freezing Temperatures Workshop, Phoenix, Arizona,* http://www1.eere.energy.gov/hydrogenandfuelcells/fc_freeze_workshop.html (2005).
5. S. D. Knights, K. M. Colbow, J. St-Pierre, D. P. Wilkinson, *Journal of power sources*, **127**, 127 (2004).
6. M. Oszcipok, D. Riemann, U. Kronenwett, M. Kreideweis, A. Zedda, *Journal of power sources,* **145**, 407 (2005).
7. E. L. Thompson, J. Horne, W. Gu, H. A. Gasteiger, *J. Electrochem. Soc.*, **155(6)**, B625 (2008).
8. S. Ge, C. Y. Wang, *J. Electrochem. Soc.*, **154(12)**, B1399 (2007).
9. PRIMEA and GORE are trademarks of W. L . Gore & Associates, Inc.
10. Certain trade names and company products are mentioned in the text or identified in an illustration in order to adequately specify the experimental procedure and equipment used. In no case does such identification imply recommendation or endorsement by the National Institute of Standards and Technology, nor does it imply that the products are necessarily the best available for the purpose.
11. M. A. Hickner, N. P. Siegel, K. S. Chen, D. N. McBrayer, D. S. Hussey, D. L. Jacobson, M. Arif, *J. Electrochem. Soc.,* **153(5)**, A902 (2006).
12. Y. Ishikawa, T. Morita, K. Nakata, K. Yoshid, and M. Shiozawa, *J. Power Sources*, **163**, 708 (2007).